Miniaturized Silicon Micromachined Bandpass Filter

육 종 관

Jong-Gwan Yook

Abstract

An extensive study on miniaturized bandpass filter(BPF) appropriate for mobile communication systems is presented in this paper. The miniaturization has been accomplished by incorporating low-loss high-index materials inside a resonating cavity fabricated in silicon substrate using micromachining etching techniques. By use of materials with dielectric constant $\varepsilon_r = 500$, filters with volume less than 0.11 mm^3 have been designed at the center frequency of 5.8 GHz with 3.3 % bandwidth. The electrical performances and design tolerances of these filters for a variety of materials and shapes are discussed and design guidelines are presented herein.

I. Introduction

In mobile communication systems, size, weight and performance are critical trade-offs in system design. In conventional designs on printed circuit boards, several discrete components can be easily identified that take quite large real estate and thus prevent high-density integration. Many RF components such as antennas, duplexers, and bandpass filters are historically considered as the most problematic elements in terms of high-density integration. In view of the above, we have focused on the miniaturization of a bandpass filter to the point where the achieved size allows for high level integration.

The proposed filter designs incorporating high-ndex materials can be realized by use of silicon/aAs micromachining or low temperature cofired ceramic(LTCC) technology. Historically silicon micromachining has been developed from the MEMS Micro-Electro-Mechanical System) community and has been recently introduced to microwave and millimeter-wave circuit and antenna applications. The application of this technology in high frequency circuits and antennas has resulted in low-loss high-performance transmission lines, high-Q (high-quality) factor filters and other passive components[1]~[6]. The usage of high resistivity silicon material has special advantages due to its compatibility with active and passive circuits. With this technology a high-Q resonator has been demonstrated recently[7] and has indicated a possibility of realizing a cavity with Q close to 600. One foreseeable disadvantage of this approach is the large lateral size of the resonator due to the air-micromachined cavity employed in the design. In this paper, as illustrated in Fig. 1 and Fig. 2 the

광주과학기술원 정보통신공학과(Dept. of Information and Communications, Kwang-Ju Institute of Science and Technology)

· 논 문 번 호 : 990826-04S

· 수정완료일자 : 1999년 9월 2일

above concept is extended to build miniaturized high-Q bandpass filters by appropriate use of high-index materials in conjunction with the micromachined cavity.

For the modeling and sensitivity analysis of the filter geometry, three dimensional finite difference time domain(FDTD) method based on the leap-frog Yee's scheme has been developed and employed. This method has allowed accurate prediction of the filter performance in wide frequency range as well as the optimization of filter geometry for a given performance target.

Ⅱ. Filter Design and Modelling

Filter design is based on the use of an integrated micromachined cavity filled with high-index material as shown in Fig. 1 and Fig. 2. It consists of input and output microstrip lines, two coupling slots in the lower interface layer and micromachined metal cavity filled with high-index dielectric material. The resonant frequency of metal cavity is well defined and can be computed through an eigenvalue analysis for arbitrary shape and material composition. Such a cavity may exhibit a high quality factor, depending on the loss tangent of dielectric material, conductivity of the metal walls as well as radiation loss from the input and output feeding network. In this study, several readily available low loss high-index materials(ε_r = 60, 200, 500) such as barium strontium titanate [8] have been considered. The losses due to finite conductivity of metal surface and complex dielectric constant have not been included in the simulations.

As mentioned earlier these filters are integrated with a microstrip feeding network as depicted in

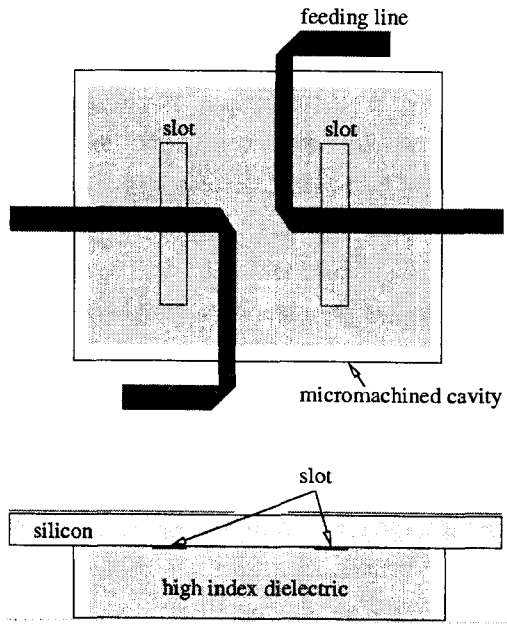

Fig. 1. Microstrip-fed slot-coupled micromachined bandpass filter.

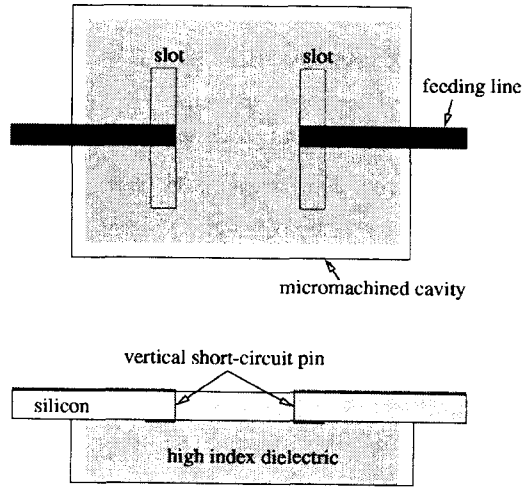

Fig. 2. Microstrip short-circuit-fed micromachined bandpass filter.

Fig. 1 and Fig. 2. In this arrangement, the feeding structure is made of a 50 Ω microstrip input/output line(80 μm wide on 100 μm thick silicon substrate) that excites the cavity through slots via

electromagnetic coupling. There are two feeding mechanisms we have considered in this study. In the first one, the microstrip line extends $\lambda g/4$ long from the slot to maximize magnetic field at the slot position. In the second approach the $\lambda g/4$ long microstrip lines are replaced with vertical short-circuit pins as shown in Fig. 2. With short circuit pins in place of the open stubs, the overall size of the filter has been significantly reduced. The electrical performance of these two geometries are compared in the next section. Table 1 summarizes the geometrical and material parameters for five different filter configurations designed for f_0 = 5.8 GHz. In all cases, the thickness and the dielectric constant of the silicon substrate is 100 μm and ε_r = 11.7, respectively. Also the coupling slot is 1200 μm long and 200 μm wide and placed one quarter of cavity length from the sides unless specified.

In terms of modeling effort, the FDTD code has been validated with the published results for the case of an empty cavity in[7] in addition to in house developed FEM code. It is worth noticing that modeling of low-loss high-Q resonant structures with time domain tools requires relatively large number of time steps to be able to extract stable frequency domain characteristics. In our simulations, 80,000 to 100,000 time steps are found necessary for convergent results.

Table 1. Geometrical and material parameters for micromachined bandpass filter. w, l, and h represents width, length, and height of cavity.

BPF	ε_r	w [mm]	l [mm]	h [mm]	Area [mm^3]
1	500	1.36	1.6	0.25	2.176
2	500	1.36	1.6	0.25	2.176
3	200	2.38	2.38	0.25	5.66
4	60	4.60	4.6	0.25	21.16
5	1	36.7	36.7	0.25	1347

Ⅲ. Frequency Characteristics of Filters

With ε_r = 60 and 200, microstrip-fed BPFs of center frequency 5.8 GHz are designed as summarized in Table 1 and verified as shown in Fig. 3 and Fig. 4. These two filters have 3 dB bandwidth of 220 MHz and exhibit very high rejection in the stop band region. The ripples in the S-parameter curves suggest that more time steps are necessary for more stable results. It is observed that more time steps only improve the smoothness of the curves and do not alter resonant frequency of the filters. For different filter characteristics, for example narrower or wider 3 dB bandwidth and high rejection band performance, the shape and number of cavity can be modified to achieve desired filter performance.

For BPFs with ε_r = 500 two different feeding structures (refer Fig. 1 and Fig. 2) produce similar frequency characteristics, as shown in Fig. 5 and Fig. 6, including almost identical (20 MHz off) resonant frequency and insertion loss. However, in terms of stop band characteristics, the microstrip feeding configuration reveals slightly better rejection performance. In addition the 3 dB bandwidth of the short-circuit-fed filter is 270 MHz which is 50 MHz wider than that of the microstrip-fed structure. This is mainly due to the fact that the bandwidth of the $\lambda g/4$-long microstrip feed network has affected the overall performance on top of the cavity characteristic.

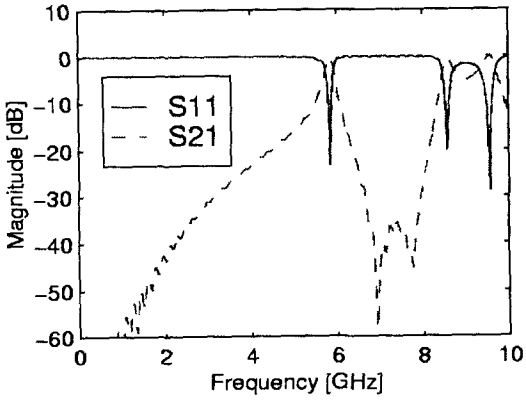

Fig. 3. Microstrip-fed BPF with $\varepsilon_r = 60$.

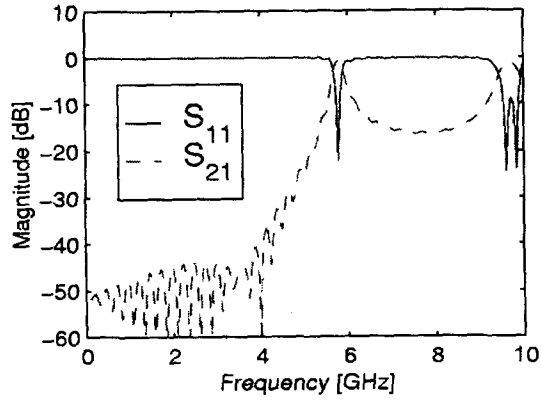

Fig. 5. Microstrip-fed BPF with $\varepsilon r = 500$.

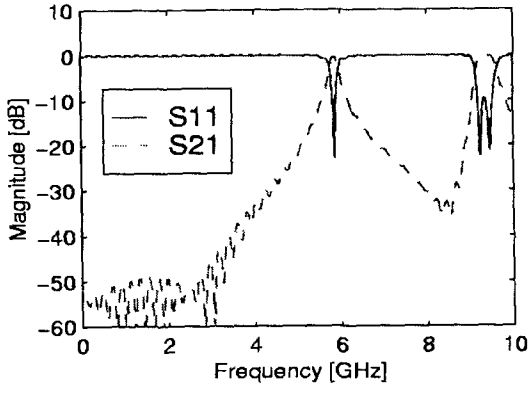

Fig. 4. Microstrip-fed BPF with $\varepsilon_r = 200$.

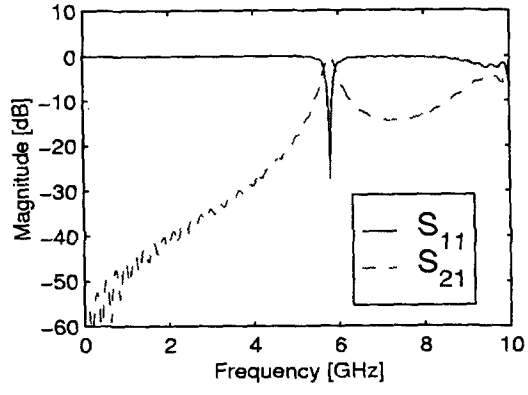

Fig. 6. Microstrip short-circuit-fed BPF $\varepsilon_r = 500$.

Ⅳ. Sensitivity Analysis

To address the manufacturing tolerance issues, extensive analysis have been performed for the effect of variety of factors, such as size and shape of dielectric material inside of the cavity, shape and position of coupling slots as well as microstrip network, cavity thickness, and even the possibility of using via holes as a replacement of cavity side walls. A comprehensive review of these investigations are discussed in the section.

4-1 Slot Width

In general, longer slot causes greater coupling between the input and output ports unless it starts to support radiating mode in the slot. In this study, while the slot length is fixed to optimum value (1,200 μm), slot width has been varied from 80 μm to 320 μm and the resulting frequency responses of the filter are observed. As summarized in Fig. 7, the resonant frequency is not a simple function of slot width, rather it has local minimum at a certain value. It is worth to mention that the overall frequency responses reveal very similar in all cases, even though wide slot exhibits slightly better performance(smaller insertion loss) and

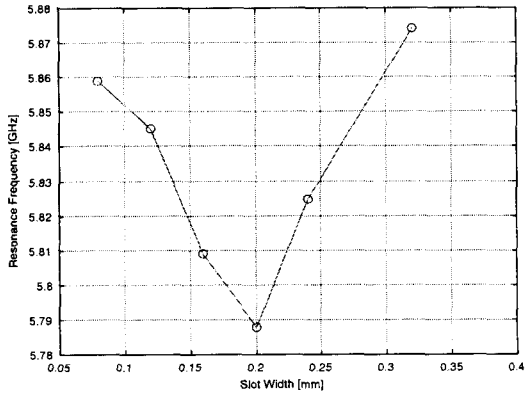

Fig. 7. Resonant frequency versus slot width.

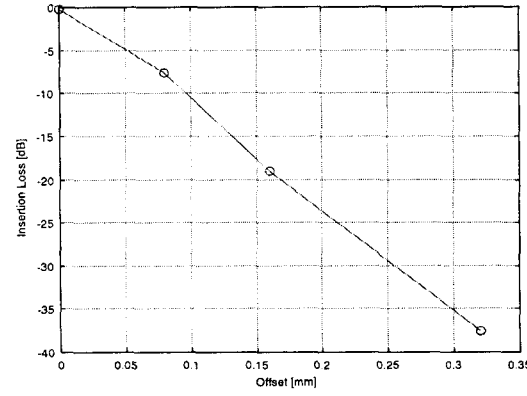

Fig. 8. Insertion loss versus feeding line offset.

wider 3 dB bandwidth.

4-2 Feeding Line Offset

To examine the effect of feeding line offset (distance from the center of the slot), various cases have been tested and the results are plotted in Fig. 8. It is observed that the insertion loss is greatly increased as the offset increases, thus suggesting center feeding is optimum in this type of structure. It is also noted that the resonant frequencies reveal negligible variations with different offset feedings. Hence it can be concluded that feeding line geometry is nearly independent of the resonant frequency of the filter, rather it strongly affects insertion loss of the filter.

4-3 Cavity Thickness

Theoretically [9], the thickness of the cavity should not affect the frequency characteristic of the dominant mode in the rectangular cavity. However, from the full-wave time domain simulations it has been turned out that the resonant frequency as well as the insertion loss characteristics heavily depend on the cavity thickness as depicted in Fig. 9. In other words, the resonant frequency of the filter moves to higher frequency region as the cavity thickness increases. Furthermore, the insertion loss of the filter gradually decreases as the cavity thickness increases and approaches to certain value as shown in the figure. Therefore, thicker cavity will provide better filter performance than the thinner one. The filter thickness, however, is limited by the thickness of the overall geometry and substrate thickness as well as etching capability. In addition, when the thickness of the cavity becomes comparable to the horizontal size of the cavity, higher order modes will be excited in near the fundamental mode, thus deteriorating the filter performance.

4-4 Dielectric Shape

The material inside of the cavity can be placed by inserting a dielectric brick having different relative dielectric constant and as a result it may not fit into the cavity exactly. In this section, the effect of the shape of the dielectric material inside of the cavity on the electrical characteristics of the

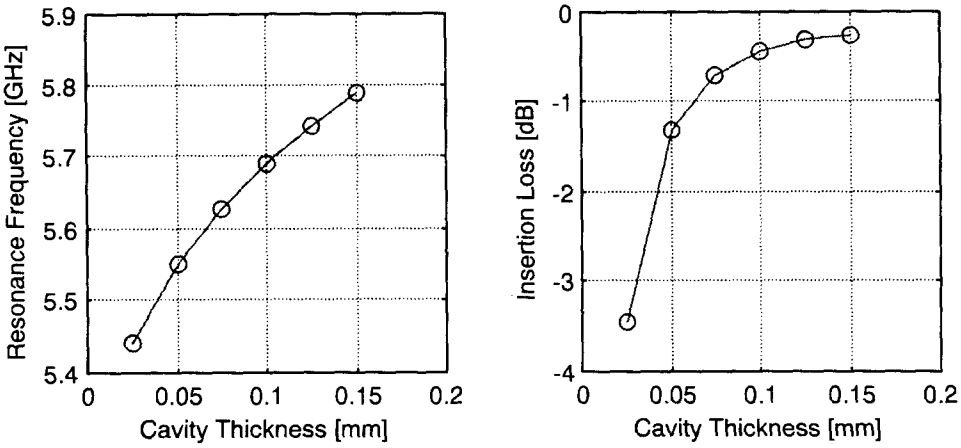

Fig. 9. Resonant frequency and insertion loss versus cavity thickness.

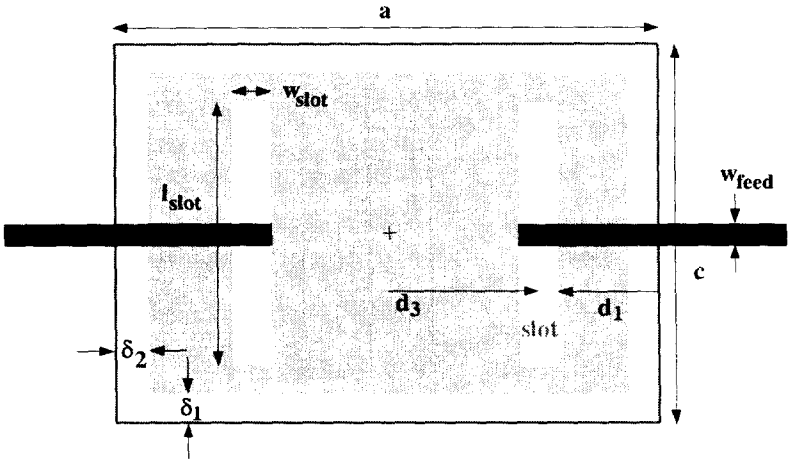

Fig. 10. Top view of the filter with dielectric material inside of the cavity.

filter will be considered. As shown in Fig. 10, δ_1 and δ_2 represent the gap distances between dielectric material and cavity side walls. δ_1 and δ_2 have been varied from 0 to 320 μm and resulting frequency responses are summarized in Fig. 11 and Fig. 12. It is apparent that as the gap sizes (δ_1 and δ_2) increase the resonant frequency increases. The relative frequency shift due to δ_1, however, is much stronger than that of δ_2, suggesting that when the filter is being fabricated, the accuracy on the dielectric dimension in lateral direction is very important.

V. Conclusions

In this paper, miniaturized silicon micromachined bandpass filters have been designed and optimized with FDTD full-wave technique. With low-loss high-index dielectric material, size of less than 2.2 mm^2 BPFs have been designed for center fre-

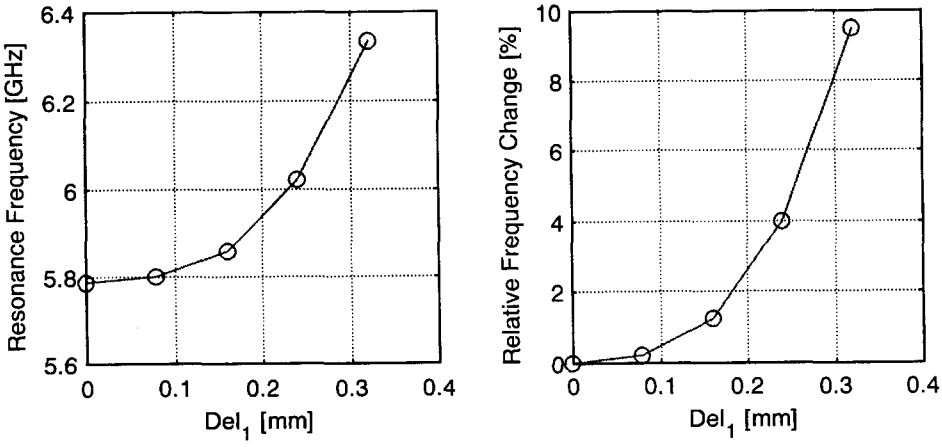

Fig. 11. δ_1 versus resonant frequency of BPF.

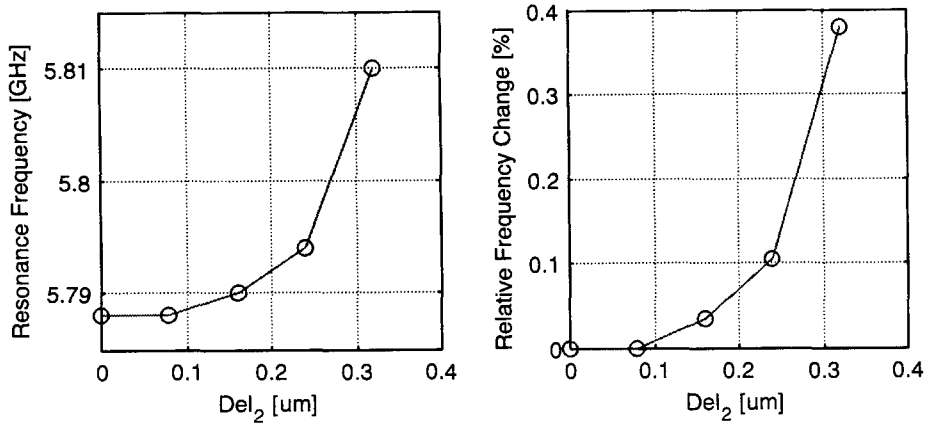

Fig. 12. δ_2 versus resonant frequency of BPF.

quency 5.8 GHz. These types of filters can be implemented using low temperature cofired ceramic (LTCC) as well as silicon micromachining technique, and eventually can be integrated into MMIC circuits providing compact-size microwave and millimeter-wave systems. One of the potential problems with this technology is the temperature sensitivity of the materials. However, this problem may easily be alleviated with recent advances in material science. For the fabrication and manufacturing tolerances, the effects of various design factors, such as shape and position of coupling slots, feeding network, cavity thickness and shape of dielectric material inside of the cavity, are extensively studied and summarized for design engineers.

References

[1] T. Weller, L. Katehi and G. Rebeiz, "High performance microshield line components," *IEEE Trans. Microwave Theory Tech.*, vol.

43, pp. 534--543, Mar., 1995.

[2] S. Robertson, L. Katehi and G. Rebeiz, "Micromachined W-band filters," *IEEE Trans. Microwave Theory Tech.*, vol. 44, pp. 598-606, Apr. 1996.

[3] T. Weller, K. Herrick and L. Katehi, "Quasi-static design technique for mm-wave micromachined filters with lumped elements and series stubs," *IEEE Trans. Microwave Theory Tech.*, vol. 45, pp. 931-938, June, 1997.

[4] R. Drayton, L. Katehi, "Development of self-packaged high frequency circuits using micromachining techniques," *IEEE Trans. Microwave Theory Tech.*, vol. 43, pt. 1, pp. 2073-2080, Sep., 1995.

[5] V. Milanovic, M. Gaitan and E. Bowen, "Micromachined microwave transmission lines in CMOS technology," *IEEE Trans. Microwave Theory Tech.*, vol. 45, pt. 1, pp. 630-635, May, 1997.

[6] I. Papapolymerou, R. Drayton and L. Katehi, "Micromachined Patch Antenna," *IEEE Trans. Antennas Propagat.*, vol. 46, pp. 275-283, Feb., 1998.

[7] I. Papapolymerou, J.-C. Cheng, J. East and L. Katehi, "Micromachined high-Q X-band resonator," *IEEE Microwave and Guided Wave Letters*, vol. 7, N. 6, pp. 168-170, June, 1997.

[8] M. Klee, U. Mackens, R. Kiewitt and G. Greuel, C. Metzmacher, "Ferroelectric Thin Films for Integrated Passive Components," *Philips J. Res.*, vol. 51, no. 3, pp. 363-386, 1998.

[9] R. F. Harrington, Time-Harmonic Electromagnetic Fields, McGraw-Hill, 1961.

Jong-Gwan Yook(S'86, M'97)

was born in Korea. He received the BS and MS degrees in Electronic Engineering from Yonsei University, Seoul, Korea, in 1987 and 1989, respectively, and Ph.D. degree from the University of Michigan, Ann Arbor, Michigan, in 1996.

Currently he is an Assistant Professor at the Kwang-Ju Institute of Science and Technology(K-JIST), Korea. His main research interests are in the area of theoretical/numerical electromagnetic modeling and characterization of microwave/millimeter-wave circuits and components and VLSI and MMICs interconnects using frequency and time domain full-wave methods, and development of numerical techniques for analysis and design of high-speed high-frequency circuits with emphasis on parallel/super computing and wireless communication applications.